Journal of Materials Chemistry C

RSCPublishing

COMMUNICATION

# Ion Conductive Properties in Ionic Liquid Crystal Confined in Porous Membrane

Cite this: DOI: 10.1039/xoxxoooooox

Y. Uchida,[a,b] T. Matsumoto,[a] T. Akita[a] and N. Nishiyama[a]

Received ooth January 2012,
Accepted ooth January 2012

DOI: 10.1039/xoxxoooooox

www.rsc.org/

**Liquid crystalline (LC) phases under nanoconfinement are known to exhibit exotic molecular orientational structures and phase transition behaviours. Here, we report the anisotropic ion conductivity and phase transition behaviours of ionic LC samples confined in aluminum oxide membranes with cylindrical pores. We found that these properties are different from the bulk ionic LC samples and depend on the molecular alignment on the pore walls.**

## Introduction

Ionic liquid crystalline (LC) materials exhibit anisotropic ion transport derived from the anisotropy of the molecular orientational ordering in LC phases.[1] For example, smectic A (SmA) phases, which ionic LC materials quite often show, form well-defined layer structures, and the molecules are oriented along the layer normal. Ionic SmA materials are microscopic phase-segregated into two regions; one is the regions with ionic groups and the other is those with non-polar alkyl chains.[1] Since the layer structure in the SmA phase of ionic compounds generates planar ion paths consisting of the ionic groups, the ion conductivity along the smectic layer plane ($\sigma_{\parallel}$) is higher than that along the layer normal ($\sigma_{\perp}$); two-dimensional (2-D) ion conduction.[2] Besides, columnar and cubic phases of ionic materials show one-dimensional (1-D)[3] and three-dimensional (3-D)[4] ion conduction derived from ion channels consisting of their ionic groups, respectively. The ion-conductive channels can be immobilized and stabilized by the polymerization after self-assembling formation of the channels in the polymerizable ionic LC materials, and such polymer films have already found a fit in many applications.[1-4] They are promising materials for fabricating flexible devices.[1] Since the previously-reported anisotropic ion-conduction systems were derived from the symmetry intrinsic to the LC phases, their formation needs highly sophisticated molecular design and fabrication technique so far.

One can control the molecular orientation of LC materials by means of anchoring effects realized by surface treatment. For example, patterned fine-tuned surfaces enable the multi-domain alignment in liquid crystal displays.[5] Since LC phases are fluid and their director field is bendable to some extent, we can also control 2-D or 3-D director field by introducing them into narrow regions surrounded by curved surfaces.[6] If an SmA material with the above-mentioned layer structure of the ionic groups is confined in spatially connected tubes in any support films and is homeotropically aligned on the walls of the tubes, ionic groups should form linear or tubular aggregates parallel to the tubes. Ion conductive properties of the ordinary ionic LC materials showing an SmA phase confined by the tubes are expected to no longer show simple 2-D ion conduction; instead, the tubes could work as ion-conductive channels in the 1-D or 3-D ion-conductive films consisting of ionic LC materials.[3,4] The composite systems consisting of LC and porous materials enable us to design the topological structure of the ion-conductive channel separately from the symmetry intrinsic to the LC phases. Thus, in contrast to the previously-reported ion-conductive polymer films, the composite systems could be composed of a variety of ionic LC compounds and support films with spatially connected tubes. Although the nanoconfinement effects of random mesopores on ionic LC phases have been reported,[7] as far as we know there have been no previous researches about nanoconfinement effects of cylindrical pores on the ion conductive properties of any ionic SmA materials.

In this paper, we discuss the ion conductivity and phase transition behaviours of an ionic SmA compound introduced into surface-treated inorganic membranes with cylindrical pores.

## Results and discussion

First, we prepared 1-hexadecyl-3-methyl-imidazolium hexafluorophosphate ([$C_{16}$mim][$PF_6$]) as the ionic material showing an SmA phase and exhibiting anisotropic ion conduction from 1-hexadecyl-3-methyl-imidazolium chloride according to the procedure written in ref. 8.

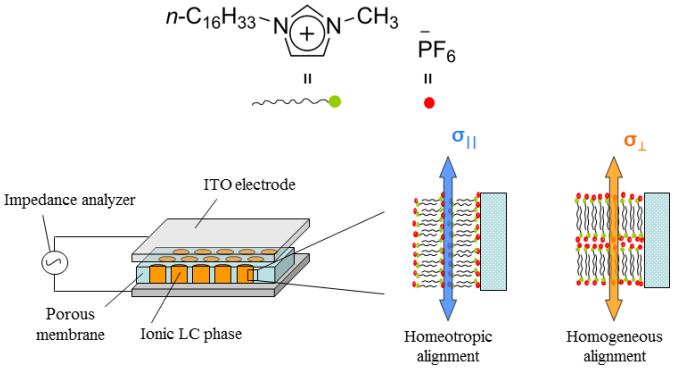


Fig. 1 Molecular structure of [$C_{16}$mim][$PF_6$] and the experimental setup of ion conductivity measurements for composite membranes.

Then, we confirmed the phase transition behaviour by differential scanning calorimetry (DSC), polarized optical microscopy (POM), and Xray diffraction (XRD) measurements. DSC charts for bulk [$C_{16}$mim][$PF_6$] showed endothermic peaks at 74.6°C and 125.2°C in the heating run, and exothermic peaks at 121.7°C and 63.8°C in the cooling run as shown in Fig. S1, corresponding to the previously-reported crystalline (Cr)-to-SmA and SmA-to-isotropic (Iso) phase transitions, and Iso-to-SmA and SmA-to-Cr phase transitions, respectively.[8] Bulk [$C_{16}$mim][$PF_6$] showed a fan-shaped texture typical for SmA phases at 90°C by POM (Fig. 2). XRD measurements for the SmA phase of bulk [$C_{16}$mim][$PF_6$] gave only one peak ($2\theta$ = 2.55°, 36.0 Å) as shown in Fig. S2. To identify the molecular stacking manner in the SmA phase, which could affect ion conductivity, we performed DFT calculations for $[C_{16}mim]^+$ ion. The DFT calculations at B3LYP/6-31G** level using Gaussian 09 program package[9] show that the longest radius of the molecular ellipsoid of $[C_{16}mim]^+$ ion ($l_{MO}$ = 33.6 Å)[10] is smaller than the layer spacing obtained from the XRD measurement ($d$) and larger than $d$/2. These results indicate that the SmA phase of [$C_{16}$mim][$PF_6$] is an interdigitated bilayer SmA phase.[11]

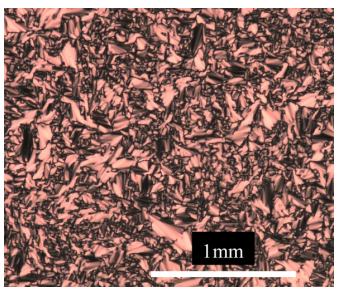


Fig. 2 Polarized optical micrographs showing a fan-shaped texture at 80°C, for [$C_{16}$mim][$PF_6$]. The scale bar at the lower right corresponds to 1 mm.

As a reference, we measured the anisotropic ion conductivities of bulk [$C_{16}$mim][$PF_6$] by introducing the sample into thin glass cells that consist of two indium tin oxide coated glasses covered with rubbed polyvinyl alcohol (PVA) films or hexadecyltrimethyl-ammonium bromide ($C_{16}$TAB) films to realize homogeneous or homeotropic surface alignment. The ion conductivities gradually increased with increase in temperature in the SmA phase in all cases as shown in Fig. 3. This is because that the viscosity of [$C_{16}$mim][$PF_6$] decreases with increase in temperature. And, conductivity along the smectic layer ($\sigma_{||}$) is larger than that along the layer normal ($\sigma_{\perp}$) in the SmA phase. These results are consistent with the previous reports.[2]

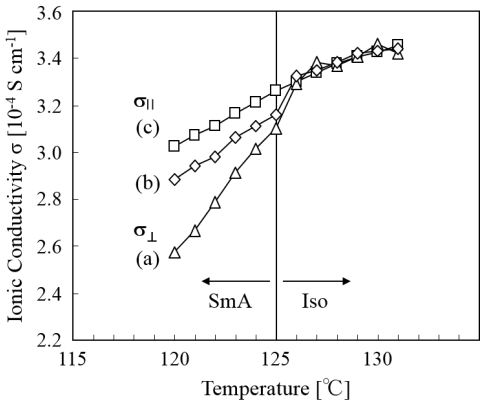


Fig. 3 Ion conductivities for ionic LC samples introduced into the ITO glass cells (a) treated with PVA, (b) untreated and (c) treated with $C_{16}$TAB.

Next, to clarify nanoconfinement effects, [$C_{16}$mim][$PF_6$] was introduced into commercially available aluminum oxide membranes (60 μm thickness) with well-defined cylindrical pores (about 100 nm diameter) aligning along the membrane normal (Fig. 1). Before the introduction of the materials, the inorganic porous membranes were surface-treated with PVA or $C_{16}$TAB to obtain homogeneous or homeotropic surface alignment on the pore walls (See Experimental section). In addition, we prepared untreated inorganic porous membranes for comparison. And we confirmed the phase transition behaviours by DSC and XRD measurements. DSC chart for [$C_{16}$mim][$PF_6$] confined in the pores shows no peaks around the SmA-to-Iso phase transition temperature as shown in Fig. S3. The heat of the SmA-to-Iso phase transition is likely to be extremely reduced in the composite membrane due to the influence of nanoconfinement in the pores. And for the XRD measurements, the composite membranes are put on the stage to be parallel to the stage. XRD patterns for the SmA phase of [$C_{16}$mim][$PF_6$] confined in the pores at 90°C show peaks at 2.45° corresponds to an SmA layer spacing of 33.0 Å as shown in Fig. S4. This layer spacing is similar to that for the bulk sample; the layer structure remains even after the confinement in the pores. The peak intensity for the SmA phase in the membrane treated with PVA is the highest, and that for the SmA phase in the membrane treated with $C_{16}$TAB is the lowest. Since the ordered structure normal to the membrane surface contributes the peak, the treatment with PVA or $C_{16}$TAB is likely to successfully give rise to homogeneous or homeotropic surface alignment as illustrated in Fig. 1. Especially in the case with the homogeneous surface alignment derived from the PVA coating, molecular director is not in a plane perpendicular to the pores but parallel to the pores. It should be because the SmA layers avoid bend deformation.

The difference in the molecular director field in the SmA phases in the composite membranes should definitely make a difference in the ion conductivity. Thus, we measured temperature dependence of ion conductivities along the membrane normal for the three composite membranes as shown in Fig. 4. For the two composite membranes with pore walls treated with $C_{16}$TAB and with untreated pore walls (Fig. 4a,b), the ion conductivities in the SmA phase are higher than that of the bulk samples, and the ion conductivities decreased at the transition from the SmA phase to the isotropic phase unlike the bulk samples. These differences in the temperature dependence of the conductivities are likely to come from the nanoconfinement effects. Layer structure is likely to be stabilized by the $Al_2O_3$ membrane. The ion conductivity of the composite membrane with pore walls treated with $C_{16}$TAB at the

 

temperature the bulk [$C_{16}$mim][$PF_6$] shows the SmA phase is higher than that of the composite membrane with pore walls treated with PVA (Fig. 4a,c). It is because the ion conductivity $\sigma_{\parallel}$ is higher than $\sigma_{\perp}$ in the SmA phases.

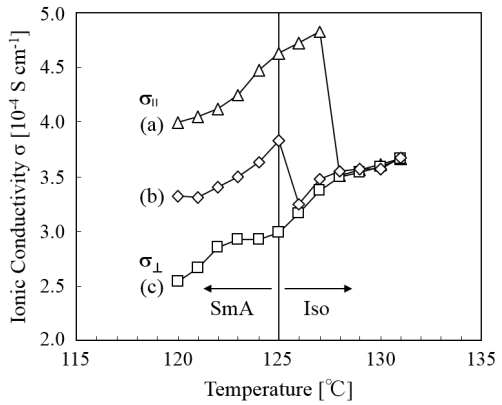


Fig. 4 Ion conductivities for ionic LC samples introduced into the porous membranes (a) treated with $C_{16}$TAB, (b) untreated and (c) treated with PVA.

In general, phase transition behaviours are influenced by the surface alignment in the nanometer-scale pores.[12] In fact, we found that the nanoconfinement also affects the transition temperature. For the composite membrane with pore walls treated with $C_{16}$TAB, the peak position of the ion conductivity is about 4°C higher than that for the other samples as shown in Fig. 4a. This suggests that in spite of the splay deformation of the director field, the SmA phase was stabilized. Although nanoconfinement effects on the phase transition temperature of liquid crystalline phases have often been reported,[13] as far as we know the increase of the LC-to-Iso phase transition temperature has never been reported. This point will be studied in the near future.

## Conclusions

We successfully fabricated ion-conductive channels by introducing ionic liquid crystals into surface-treated inorganic porous membranes, whose ion conductivities depend on the surface treatment on the pore walls. A huge variety of 2-D and 3-D director fields realized in LC colloids and LC emulsions[14] are promising scaffolds for the new ion channels. In addition, our results indicate that the switching of the director using external fields or light enable us to control the ion conductivity. Moreover, since phase transition temperature increases due to nanoconfinement is unusual behaviour, these system might exhibit other peculiar properties unlike previously-reported physical properties for embedding LC materials in nanoporous and mesoporous substrates.[6,13]

## Experimental section

The inorganic aluminum oxide membrane with a pore diameter of 100 nm (Anopore: Whatman)[15] was immersed in 0.1 wt% aqueous polyvinyl alcohol (PVA: molecular weight of 66,000 from Wako, and molecular weight distribution and end groups are not disclosed) solution or 1 wt% aqueous hexadecyltrimethylammonium bromide ($C_{16}$TAB) solution to obtain homogeneous or homeotropic surface alignment for an hour. Then, the treated membranes were dried at 180°C for an hour. The treated membranes were completely filled with [$C_{16}$mim][$PF_6$] by capillary action at 140°C, where it exhibits the isotropic phase. Excess [$C_{16}$mim][$PF_6$] was wiped away from the membrane surface with a filter paper. For each measurement, we cooled the samples with the cooling rate of 0.1°C/min, after heating the sample to 130°C where the sample showing isotropic phase. Ion conductivities for the composite membranes were measured along the membrane normal with the experimental setup shown in Fig. 1; the composite membranes were sandwiched between two ITO glass plates coated with PVA. To measure the conductivity of the bulk sample, we introduced [C16mim][PF6] into cells consisting of two ITO glass plates coated with PVA or $C_{16}$TAB and 10 μm particles as a spacer. We performed POM (BX60: Olympus), XRD analysis using Cu-Kα radiation with 1.5418 Å (X'PERT MPD: Philips), DSC (DSC-60: Shimadzu) and ion conductivity measurements by impedance analyser (SI 1260: Toyo corp.) for bulk [$C_{16}$mim][$PF_6$] introduced into glass cells and for composite membranes with [$C_{16}$mim][$PF_6$]. The membrane pieces were placed in the DSC pans and 1~2 mg of the ionic LC material was contained in the membrane in a single DSC measurement. This amount is enough to obtain the DSC peak of ordinary SmA-to-Iso phase transition.

## Acknowledgements

We thank Professor Takashi Kato, The University of Tokyo, for helpful advice. This work was supported in part by the Japan Science and Technology Agency (JST) 'Precursory Research for Embryonic Science and Technology (PRESTO)' for a project of 'Molecular technology and creation of new function' and by Foundation for Promotion of Material Science and Technology of Japan (MST Foundation).

## Notes and references

[a] Graduate School of Engineering Science, Osaka University, 1-3 Machikaneyama-cho, Toyonaka, Osaka, 560-8531, Japan. E-mail: yuchida@cheng.es.osaka-u.ac.jp.

[b] JST, PRESTO, 4-1-8 Honcho, Kawaguchi, Saitama, 332-0012, Japan.

† Electronic supplementary information (ESI) available: DSC curves and XRD patterns for bulk [$C_{16}$mim][$PF_6$] and composite membranes. See DOI: 10.1039/c000000x/

1 J. W. Goodby, P. J. Collings, T. Kato, C. Tschierske, H. Gleeson, P. Raynes, Handbook of Liquid Crystals, 2nd ed.; Wiley-VCH: Weinheim, 2014; T. Kato, *Science*, 2002, **295**, 5564; K. Binnemans, *Chem. Rev.*, 2005, **105**, 4148.

2 M. Yoshio, T. Mukai, K. Kanie, M. Yoshizawa, H. Ohno, T. Kato, *Chem. Lett.*, 2002, **31**, 320; M. Yoshio, T. Mukai, K. Kanie, M. Yoshizawa, H. Ohno, T. Kato, *Adv. Mater.*, 2002, **14**, 351; K. Hoshino, M. Yoshio, T. Mukai, K. Kishimoto, H. Ohno, T. Kato, *J. Polym. Sci., Polym. Chem.*, 2003, **41**, 3486; T. Mukai, M. Yoshio, T. Kato, M. Yoshizawa, H. Ohno, *Chem. Commun.*, 2005, 1333; N. Yamanaka, R. Kawano, W. Kubo, T. Kitamura, Y. Wada, M. Watanabe, S. Yanagida,

*Chem. Commun.*, 2005, 740; N. Yamanaka, R. Kawano, W. Kubo, N. Masaki, T. Kitamura, Y. Wada, M. Watanabe, S. Yanagida, *J. Phys. Chem. B*, 2007, **111**, 740; B. Soberats, E. Uchida, M. Yoshio, J. Kagimoto, H. Ohno, T. Kato, *J. Am. Chem. Soc.*, 2014, **136**, 9552.

3 M. Yoshio, T. Mukai, H. Ohno, T. Kato, *J. Am. Chem. Soc.*, 2004, **126**, 994; M. Yoshio, T. Kagata, K. Hoshino, T. Mukai, H. Ohno, T. Kato, *J. Am. Chem. Soc.*, 2006, **128**, 5570; H. Shimura, M. Yoshio, K. Hoshino, T. Mukai, H. Ohno, T. Kato, *J. Am. Chem. Soc.*, 2008, **130**, 1759.

4 T. Ichikawa, M. Yoshio, A. Hamasaki, T. Mukai, H. Ohno, T. Kato, *J. Am. Chem. Soc.*, 2007, **129**, 10663; T. Ichikawa, M. Yoshio, A. Hamasaki, J. Kagimoto, H. Ohno, T. Kato, *J. Am. Chem. Soc.*, 2011, **133**, 2163; T. Ichikawa, M. Yoshio, A. Hamasaki, S. Taguchi, X.-Zeng, G. Ungar, H. Ohno, T. Kato, *J. Am. Chem. Soc.*, 2012, **134**, 2634.

5 M. Schadt, H. Seiberle, A. Schuster, *Nature*, 1996, **381**, 212.

6 E. Glowacki, K. Horovitz, C. W. Tang, K. L. Marshall, *Adv. Mater.*, 2010, **20**, 2778; S. Calus, D. Rau, P. Huber, A. V. Kityk, *Phys. Rev. E*, 2012, **86**, 021701.

7 F. T. U. Kohler, B. Morain, A. Weiß, M. Laurin, J. Libuda, V. Wagner, B. U. Melcher, X. Wang, K. Meyer, P. Wasserscheid, *ChemPhysChem*, 2011, **12**, 3539.

8 C. M. Gordon, J. D. Holbrey, A. R. Kennedy, K. R. Seddon, *J. Mater. Chem.*, 1998, **8**, 2627.

9 M. J. Frisch, G. W. Trucks, H. B. Schlegel, G. E. Scuseria, M. A. Robb, J. R. Cheeseman, G. Scalmani, V. Barone, B. Mennucci, G. A. Petersson, H. Nakatsuji, M. Caricato, X. Li, H. P. Hratchian, A. F. Izmaylov, J. Bloino, G. Zheng, J. L. Sonnenberg, M. Hada, M. Ehara, K. Toyota, R. Fukuda, J. Hasegawa, M. Ishida, T. Nakajima, Y. Honda, O. Kitao, H. Nakai, T. Vreven, J. A. Montgomery, Jr., J. E. Peralta, F. Ogliaro, M. Bearpark, J. J. Heyd, E. Brothers, K. N. Kudin, V. N. Staroverov, R. Kobayashi, J. Normand, K. Raghavachari, A. Rendell, J. C. Burant, S. S. Iyengar, J. Tomasi, M. Cossi, N. Rega, J. M. Millam, M. Klene, J. E. Knox, J. B. Cross, V. Bakken, C. Adamo, J. Jaramillo, R. Gomperts, R. E. Stratmann, O. Yazyev, A. J. Austin, R. Cammi, C. Pomelli, J. W. Ochterski, R. L. Martin, K. Morokuma, V. G. Zakrzewski, G. A. Voth, P. Salvador, J. J. Dannenberg, S. Dapprich, A. D. Daniels, O. Farkas, J. B. Foresman, J. V. Ortiz, J. Cioslowski, D. J. Fox, (2009). Gaussian 09 Revision D.01, Gaussian Inc., Wallingford CT.

10 Y. Uchida, R. Tamura, N. Ikuma, S. Shimono, J. Yamauchi, Y. Shimbo, H. Takezoe, Y. Aoki, H. Nohira, *J. Mater. Chem.*, 2009, **19**, 415; Y. Uchida, S. Oki, R. Tamura, T. Sakaguchi, K. Suzuki, K. Ishibashi, J. Yamauchi, *J. Mater. Chem.*, 2009, **19**, 6877; Y. Uchida, K. Suzuki, R. Tamura, Y. Aoki, H. Nohira, *J. Phys. Chem. B*, 2013, **117**, 3054.

11 A. E. Bradlley, C. Hardacre, J. D. Holbrey, S. Johnston, S. E. J. McMath, M. Nieuwenhuyzen, *Chem. Mater.*, 2002, **14**, 629.

12 S. Kralj, G. Cordoyiannis, D. Jesenek, A. Zidansek, G. Lahajnar, N. Novak, H. Amenitsch, Z. Kutnjak, *Soft Matter*, 2012, **8**, 2460.

13 G. S. Iannacchione, D. Finotello, *Phys. Rev. Lett.*, 1992, **69**, 2094; S. Qian, G. S. Iannacchione, D. Finotello, *Phys. Rev. E*, 1998, **57**, 4305; G. Cordoyiannis, A. Zidansek, G. Lahajnar, Z. Kutnjak, H. Amenitsch, G. Nounesis, S. Kralj, *Phys. Rev. E*, 2009, **79**, 051703; S. Kralj, G. Cordoyiannis, D. Jesenek, A. Zidansek, G. Lahajnar, N. Novak, H. Amenitsch, Z. Kutnjak, *Soft Matter*, 2012, **8**, 2460.

14 P. Poulin, H. Stark, T. C. Lubensky, D. A. Weitz, *Science*, 1997, **275**, 1770; I. Musevic, M. Skarabot, U. Tkalec, M. Ravnik, S. Zumer, *Science*, 2006, **313**, 954.

15 ALLIANCE Biosystems 「ANOPORE Inorganic Aluminum Oxide Membrane Filters」 http://www.alliance-bio.com/filters/filters.html.

 